Amplitude-phase multistability in multiatomic optical systems

S. Ya. Kilin and T. B. Krinitskaya
Institute of Physics, Academy of Sciences of Belarus, F. Skorina avenue 70, 220602 Minsk, Belarus
(Received 19 October 1992)

The effect of amplitude-phase multistability in the Dicke model inside a coherently driven cavity is discussed for the case of large Rabi frequencies and a small rate of atomic decay, compared with the decay of the cavity mode. The quantum and semiclassical interpretations of the predicted effect are given on the basis of the Tavis-Cummings model and a proposed model of weakly coupled harmonic oscillators. The analytical solution is obtained for a two-atom system. The possibility of observing amplitude-phase multistability is also considered.

PACS number(s): 42.65.Pc, 42.50.Fx, 42.50.Hz

I. INTRODUCTION

Since the pioneering Dicke work [1], the problem of collective effects continues to occupy one of the central positions in quantum optics. The initial problem of the decay of the collectively emitting atoms that are located in a small volume compared with the wavelength has been generalized to include collective decay (superradiation, superfluorescence) of an extended system (see, for example, [2]).

The problem of resonance fluorescence in the Dicke model excited by a strong optical radiation was considered in [3–7]. In particular, it has been shown that for a certain value of the input field intensity, the nonequilibrium phase transition analogous with the second-order phase transition occurs [3,4]. When interatomic interactions are taken into account, the considered system can manifest the nonequilibrium phase transition of the first order, the reason for which is connected with the equivalence of the system and an anharmonic oscillator in a driven coherent field [7].

On the other hand, as has been shown in [8], the system of *independent* radiating atoms in an optical cavity displays the effect of absorptive optical bistability, for which the dependence of the output field on the input pump is equivalent to the van der Waals isotherm describing the phase transition "liquid–gas" of the first order. However, the effect of optical bistability is not a consequence of collective effects induced by coupling of atoms via cavity mode field, as described in [8]. This phenomenon is defined by a single-atom self-action effect because of atomic-state dependence on the intracavity field, which is the sum of the field created by an input pump and the field reradiated by the atom. So, in the recent publications [9–11], it has been demonstrated that a single atom in a cavity strongly interacting with a cavity mode field can display the bistable properties. Moreover, besides the known absorptive bistability (or bistability of the real part of the field amplitude) [9], a new effect of phase optical bistability can be observed [10,11]. As has been mentioned in [10], the effect of phase bistability has a simple interpretation on the basis of representation of a strongly coupled atom and an intracavity field as a single quantum system.

In the present article, we investigate an effect arising as a mutual result both of the collective-atomic-emission nature and of the atomic self-action effects in a high-Q cavity. For this purpose, we generalize a single-atom model of quantum optics [10,11] for the case of a system of two-level atoms located in a volume small compared with the resonant wavelength.

The collection of atoms involved is placed in a coherently driven high-quality optical cavity. An intracavity field mode excited by the external optical field strongly interacts with the system of atoms and decays due to the partial mirror transmission. The decay of atomic states arises from spontaneous emission into noncavity modes, which are considered here as modes of a free space.

In the present paper, we demonstrate that, for the described model (the Dicke model in driven high-Q cavity), in the case of well-separated components (large Rabi frequencies) [5] and small spontaneous transition rate compared with the decay rate of the cavity field mode, the amplitude-phase multistability takes place. The dependence of the number of stable points in the phase space of the model on the number of atoms and the spontaneous atomic transition rate is analyzed, and the conditions under which the predicted effect is observed are presented.

II. MODEL

The system of two-level atoms with resonance frequency ω confined to a region whose linear dimensions are small compared to wavelength is described by the collective Dicke operators $J_+=\sum_i \sigma_{i+}$, $J_-=\sum_i \sigma_{i-}$, $J_z=\sum_i \sigma_{iz}$ ($\sigma_{i\pm}$, σ_{iz} are the single-atom operators) satisfying the commutation relations $[J_+,J_-]=2J_z$, $[J_z,J_\pm]=\pm J_\pm$. The action of the operators $J_\pm,J_z$ on the collective Dicke states $|j,m\rangle$, where j is the maximum "energy spin" value of the system of particles ($j=N/2$, N is the number of atoms, m is the projection of "energy spin" on the z axis, $-j\le m\le j$), is defined by the well-known relations

$$J_+|j,m\rangle=\sqrt{(j+m+1)(j-m)}\,|j,m+1\rangle\ , \tag{1a}$$

$$J_-|j,m\rangle=\sqrt{(j+m)(j-m+1)}\,|j,m-1\rangle\ . \tag{1b}$$

The collective Dicke states $|j,m\rangle$ are eigenstates for the operator J_z and the operator of the total "energy spin" J^2:

$$J_z|j,m\rangle = m|j,m\rangle \ , \tag{2a}$$

$$J^2|j,m\rangle = j(j+1)|j,m\rangle \ . \tag{2b}$$

The single-mode cavity field is represented by a harmonic oscillator with frequency ω_0 and boson creation and annihilation operators $a^\dagger$ and a. The cavity mode excitation by the coherent pump with amplitude E is described by the Hamiltonian $i\hbar E(a^\dagger - a)$. The atomic system and cavity field interaction is realized via the Hamiltonian $\hbar g(a^\dagger J_- + aJ_+)$. Taking into account the atomic and the cavity field relaxation, the quantum-mechanical description of the model in terms of the reduced density matrix is given by the following master equations, written in a rotating frame:

$$\dot{\rho} = E[a^\dagger - a,\rho] - i\Delta\omega[J_z,\rho] - ig[a^\dagger J_- + aJ_+,\rho] + k([a,\rho a^\dagger] + [a\rho,a^\dagger]) + \gamma/2([J_-,\rho J_+] + [J_-\rho,J_+]) \ , \tag{3}$$

where $\Delta\omega = \omega - \omega_0$ is the atom-field frequency detuning, g is the atom-field coupling constant, γ is the rate of spontaneous emission into field modes other than the cavity mode, $k = \pi/F\tau_c$ is the cavity decay rate, with $\tau_c = 2L/c$ being the round-trip time, L is the cavity length, and F is the cavity finesse. It should be noted that, for the model (3), the conservation law of the total "energy spin" square takes place:

$$\langle J^2 \rangle = \langle J_\pm J_\mp \rangle + \langle J_2^z \rangle + \langle J_z \rangle = j(j+1) \ . \tag{4}$$

The same master equation as Eq. (3) has been used in [12] for the discussions of the influence of collective effects on absorptive optical bistability. This equation has been solved in [12] in so-called decorrelation approximation when the averages like $\langle aJ_i \rangle$ are factorized ($\langle aJ_i \rangle = \langle a \rangle \langle J_i \rangle$). But the atomic-field correlations lead to new quantum effects. It has been shown in [10,11] that these quantum correlations are the reason for the predicted effect of a single-atom phase bistability. In this paper, we solve Eq. (3) without applying for the decorrelation approximation.

In the absence of the atoms ($g = \gamma = 0$), the steady state of the intracavity field should be the coherent state with amplitude E/k. Accordingly, it is very convenient to pick it out in the explicit form from the density matrix ρ, using the displacement operator $D(E/k) = \exp[E(a^\dagger - a)/k]$,

$$\bar{\rho} = D^{-1}(E/k)\rho D(E/k) \ . \tag{5}$$

As a result, the equation for the transformed matrix $\bar{\rho}$ takes the form

$$\dot{\bar{\rho}} = -2i\vartheta[J_x,\bar{\rho}] - i\Delta\omega[J_z,\bar{\rho}] - ig[a^\dagger J_- + aJ_+,\bar{\rho}] + k([a,\bar{\rho}a^\dagger] + [a\bar{\rho},a^\dagger]) + \gamma/2([J_-,\bar{\rho}J_+] + [J_-\bar{\rho},J_+]) \ , \tag{6}$$

where the first term describes the system evolution induced by the coherent field E/k ($\vartheta = gE/k$ is the Rabi frequency), whereas the term $E[a^\dagger - a,\rho]$ corresponding to the intracavity field excitation [see Eq. (3)] is absent.

Before solving Eq. (3), it is useful to note that the operators depicting the atomic system and the single-atom two-level system realize different irreducible representations of the same group SU(2), but they satisfy the identical commutation relations. Therefore, we can apply for the multiatomic system the same canonical transformations that have been used in Ref. [8], where the single-atom optical bistability has been considered. The generalization is a simple substitution of the spin Pauli operators σ_z, $\sigma_\pm$ for the collective Dicke operators J_z, $J_\pm$.

III. LARGE RABI FREQUENCIES

The exact equation (6) can be solved approximately in the case with large generalized Rabi frequency $\Omega = [(2\vartheta)^2 + (\Delta\omega)^2]^{1/2}$. To obtain this solution, let us make the rotation transformation in the space of the vectors (J_x, J_y, J_z)

$$J_i' = \exp(-i\varphi J_y) J_i \exp(i\varphi J_y) \ , \quad i = x,y,z \ , \tag{7}$$

around the axis y on such an angle φ that $s = \sin\varphi = 2\vartheta/\Omega$, $c = \cos\varphi = \Delta\omega/\Omega$. The eigenstates $|j,m'\rangle$ of the transformed operator J_z' are expressed through the linear superposition of the old basis states $|j,m\rangle$

$$|j,m'\rangle = \sum_{m=-j}^{j} d^j_{mm'}(\varphi)|m\rangle \ , \tag{8}$$

where $d^j_{mm'}(\varphi) = \langle m|\exp(-i\varphi J_y)|m'\rangle$ is the Wigner d function [13].

Assuming Ω^{-1} as the shortest time scale of the problem comparing with $(N\gamma)^{-1}$—the collective relaxation time of the atoms, k^{-1}—the damping time of the intracavity field, and $[N/2(g^2/k)]^{-1}$—the period of the Rabi oscillations induced by the reradiated field

$$\Omega^{-1} \ll (N\gamma)^{-1}, k^{-1}, \left[\frac{Ng}{2k}\right]^{-1} \ , \tag{9}$$

we can make the transformation to the dressed-state representation for the density matrix ρ':

$$\bar{\rho} = \exp(-i\Omega J_z' t)\rho' \exp(i\Omega J_z' t) \ , \tag{10}$$

with temporal dependence of operators $J_i(t)$

$$J_+(t) = sJ_z' + \frac{1+c}{2}J_+' e^{i\Omega t} - \frac{1-c}{2}J_-' e^{-i\Omega t} \ , \tag{11a}$$

$$J_z(t) = cJ_z' - \frac{s}{2}J_+' e^{i\Omega t} - \frac{s}{2}J_-' e^{-i\Omega t} \ , \tag{11b}$$

and then average the master equation for the dressed density matrix ρ' over the fast Rabi oscillations. As a result of the averaging, we obtain the equation

$$\dot{\rho}'=-igs[(a^{\dagger}+a)J'_z,\rho']+k([a,\rho'a^{\dagger}]+[a\rho',a^{\dagger}])+\frac{\gamma s^2}{2}([J'_z,\rho'J'_z]+[J'_z\rho',J'_z])$$
$$+\frac{d_{12}}{2}([J'_+,\rho',J'_-]+[J'_+\rho',J'_-])+\frac{d_{21}}{2}([J'_-,\rho'J'_+]+[J'_-\rho',J'_+]) , \quad (12)$$

where $d_{12}=[\gamma(1-c)^2]/4$, $d_{21}=[\gamma(1+c)^2]/4$. This equation satisfies the law of the particle number conservation (4). Following the equations for the diagonal elements of the transformed and averaged density matrix ρ' (10)

$$\dot{\rho}'_{-j'-j'}=\frac{igN}{2}[a^{\dagger}+a,\rho'_{-j'-j'}]+k([a,\rho'_{-j'-j'}a^{\dagger}]+[a\rho'_{-j'-j'},a^{\dagger}])+d_{21}N\rho'_{-j'+1,-j'+1}-d_{12}N\rho'_{-j'-j} ,$$
$$\dot{\rho}'_{m'm'}=igm'[a^{\dagger}+a,\rho'_{m'm'}]+k([a,\rho'_{m'm'}a^{\dagger}]+[a\rho'_{m'm'},a^{\dagger}])$$
$$+d_{12}(j+m')(j-m'+1)\rho'_{m'-1,m'-1}+d_{21}(j+m'+1)(j-m')\rho'_{m'+1,m'+1}$$
$$-(d_{12}(j+m'+1)(j-m')+d_{21}(j+m')(j-m'+1))\rho'_{m'm'} ,$$
$$\dot{\rho}'_{j'j'}=-\frac{igN}{2}[a^{\dagger}+a,\rho'_{j'j'}]+k([a,\rho'_{j'j'}a^{\dagger}]+[a\rho'_{j'j'},a^{\dagger}])+d_{12}N\rho'_{j'-1,j'-1}-d_{21}N\rho'_{j'j'} , \quad (13)$$

the atoms belonging to the different eigenstates $|j,m'\rangle$ (8) interact independently with the resonator field at small values of the spontaneous transition probability into noncavity modes γ (at small values of d_{ij}). The equations for the diagonal elements $\rho'_{m'm'}$ coincide with the equations for damping harmonic oscillators excited by the coherent radiation whose complex amplitude ($\sim gm'$) is varied for the different oscillators. Therefore, at $d_{ij}=0$, the cavity field will have $2j+1$ possible stationary values of the amplitude:

$$\alpha_{0m'}=E/k+igm'/k \quad (m'=-j,\ldots,j) . \quad (14)$$

IV. INTERPRETATION ON THE BASIS OF THE TAVIS-CUMMINGS MODEL

The possibility of the representation of the quantum system, "field plus atoms," in the form of weak-coupling harmonic oscillators can be clarified on the basis of the Tavis-Cummings model [14] (see Appendix and Fig. 1). For this purpose, we will consider the excitation of the eigenstates of the Tavis-Cummings model by an external coherent radiation. The eigenstates of the Tavis-Cummings Hamiltonian

$$H=\hbar\omega a^{\dagger}a+\hbar\omega J_z+\hbar g(a^{\dagger}J_-+aJ_+)$$

for the case of the exact resonance are presented in the form (A2)

$$|2j,n,r\rangle=\sum_{m=-j}^{k}\alpha_m^n|n-j-m\rangle_f|m\rangle_a , \quad (15)$$

where indexes f and a mark the eigenstates of the intracavity field and the atomic system, respectively. The number n is equal to the number of the excitations in the "field plus atoms" system. The number r enumerates the eigenstates belonging to the state with the fixed excitation number n. At $n<2j$, the number k is equal to $n-j$, and r changes from $-n/2$ to $(n/2)$. At $n\geq 2j$, we have $k=j$, and r changes from $-j/2$ to $j/2$. The eigenstates of the Hamiltonian H are

$$\mathcal{E}_{zj,n,r}=\hbar\omega(n-j)+E_{2j,n,r} , \quad (16)$$

where $E_{2j,n,r}$, the eigenstates of the interaction Hamiltonian $\hbar g(a^{\dagger}J_-+aJ_+)$, yields the energy spectrum of the system. The latter can be presented as the levels of noninteracting atoms and field split by their interaction on the $n+1$ sublevel when $n<2j$ and on the $2j+1$ sublevel when $n\geq 2j$ (Fig. 1).

The external field perturbing the system "atoms plus intracavity field" [the interaction Hamiltonian $-iE(a-a^{\dagger})$] leads to the transitions between the eigenstates $|2j,n,r\rangle$. The different paths of excitation for the numerically calculated energy levels of the Tavis-Cummings system are presented in Fig. 1(a) ($N=2$) and Fig. 1(b) ($N=3$). The first two paths are starting from the ground state with the equal probability (due to the equality of frequency detunings $|\hbar\omega-\mathcal{E}_{2j,1,1/2}|$ and $|\hbar\omega-\mathcal{E}_{2j,1,-1/2}|$) exciting the states $|2j,1,\frac{1}{2}\rangle$ and $|2j,1,-\frac{1}{2}\rangle$:

$$|2j,0,0\rangle\rightarrow\begin{cases}|2j,1,\frac{1}{2}\rangle\\ |2j,1,-\frac{1}{2}\rangle\end{cases} .$$

The probability of excitation of the next states already depends on the state from which the system starts. The transitions

$$|2j,1,\tfrac{1}{2}\rangle\rightarrow|2j,2,1\rangle ,$$
$$|2j,1,-\tfrac{1}{2}\rangle\rightarrow|2j,2,-1\rangle ,$$

are more probable because of smaller frequency detuning compared with other transitions. With increasing n, the situation is repeated. When $n\geq 2j$, the most probable transitions for these two paths are those made without changing the number r:

$$|2j,n,j\rangle\rightarrow|2j,n+1,j\rangle ,$$
$$|2j,n,-j\rangle\rightarrow|2j,n+1,-j\rangle .$$

From this point of view, the two first excitation paths can be depicted as

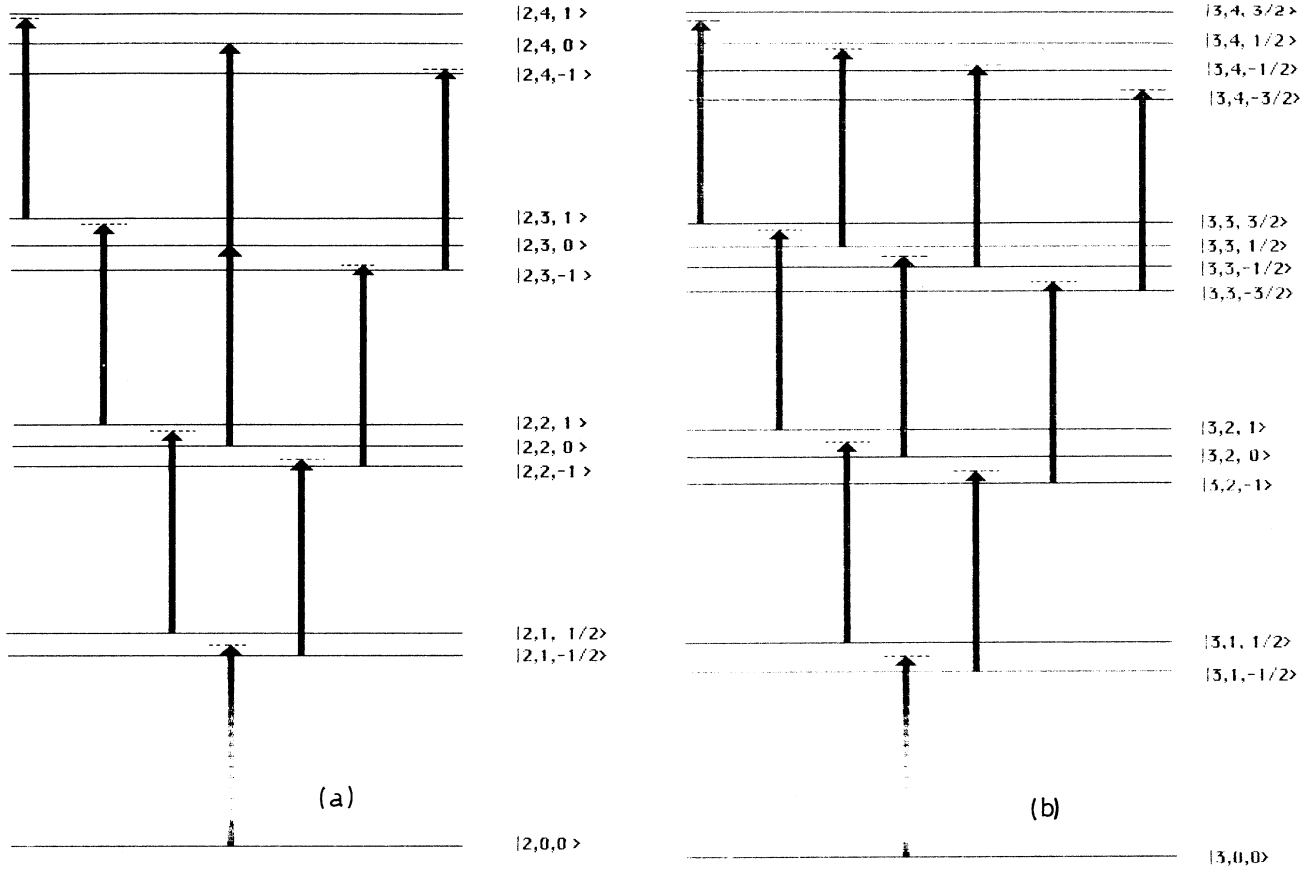

FIG. 1. Forming of the independent excitation paths in the Tavis-Cummings model under the action of a resonant classic field. Numerical calculations have been done on the basis of Eqs. (A5)–(A7) when N is even [$N=2$ (a)], or odd [$N=3$ (b)].

$$|2j,0,0\rangle \rightarrow \begin{cases} |2j,1,\frac{1}{2}\rangle \rightarrow |2j,2,1\rangle \rightarrow \ldots \rightarrow |2j,n,j\rangle \rightarrow |2j,n+1,j\rangle \rightarrow \ldots \\ |2j,1,-\frac{1}{2}\rangle \rightarrow |2j,2,-1\rangle \rightarrow \ldots \rightarrow |2j,n,-j\rangle \rightarrow |2j,n+1,-j\rangle \rightarrow \ldots \end{cases} \tag{17}$$

The next series is beginning from the state corresponding to the two excitations in system ($n=2$) and number $r=0$: $|2j,2,0\rangle$. The forming of one (at $2j=2$ [Fig. 1(a)]) or two (at $2j>2$ [Fig. 1(b)]), new excitation paths started from the state $|2j,2,0\rangle$ proceed analogously to the creation of paths (17). Thus, every state $|2j,2l,0\rangle$, where l is integer and $2l<2j$, gives rise to the new excitation paths. The general number of excitation paths picked out in such a way coincides with the maximum number of the split energy levels belonging to the same n and equals $2j+1$.

As shown in the Appendix, at the large excitation numbers $n \gg 2j$, the eigenstates of the Tavis-Cummings Hamiltonian can be represented in the factorized form

$$|2j,n,r\rangle \approx |n\rangle_f |r\rangle_\alpha , \tag{18}$$

where the states $|r\rangle_\alpha = \sum_{m=-j}^{j} d^j_{mr}(-\pi/2)|m\rangle_\alpha$ coincide with the "dressed" states (8) at $\varphi=-\pi/2$. Besides that, in accordance with Eq. (16) and at $n \gg 2j$, the eigenstates of energy are equal to

$$\mathcal{E}_{2j,n,r} = \hbar\omega(n-j)+2\hbar g\sqrt{n}\, r , \tag{19}$$

i.e., the detuning of the transition frequency

$$|2j,n,r\rangle \rightarrow |2j,n+1,r\rangle$$

is decreased for each chosen rth excitation path with the increasing n.

Therefore, according to (18), the eigenstates of the operator J_x given by Eq. (8) are the dressed atomic states defining, at $n \gg 2j$, the quasiclassical eigenstates of the Tavis-Cummings Hamiltonian. Using these states as a basis, we have obtained Eqs. (13) representing the excitation of the system "atoms plus intracavity field" as the evolution of $2j+1$ weakly coupled oscillators. This representation is equivalent to the choosing of $2j+1$ independent excitation paths at large n in the Tavis-Cummings model.

The atomic relaxation in this model results in the transitions from one chosen path to another. In Eqs. (13), these transitions are described by the terms containing

the spontaneous transition rates d_{21}, d_{12}. In accordance with Eqs. (13), the random quantum jumps are allowed between the states of neighbor harmonic oscillators with the probabilities proportional to the quantities $d_{12}(j+m')(j-m'+1)$ and $d_{21}(j+m'+1)(j-m')$. With the decreasing of the transition probabilities, the cavity field will spend most of the time in the state with one of the amplitudes (14) while the atomic system will be at the corresponding state $|j,m'\rangle$. It enables us to describe the multistability effect in the considered system. The quantitative estimation of the lifetime in the fixed state will be given in Sec. VII.

V. NUMERICAL SOLUTION

To solve numerically Eqs. (13), we use the characteristic matrix

$$\mathcal{J}_{m'n'}=\mathrm{Sp}[\exp(\lambda a^{\dagger})\exp(-\lambda^* a)D(E/k) \times\rho'_{m'n'}D^{-1}(E/k)] . \tag{20}$$

In the dressed-state basis, the system of equations for $\mathcal{J}_{m'n'}=\langle j,m'|\mathcal{J}|j,n'\rangle$ obtained from Eqs. (13) breaks up into two independent subsystems for the diagonal and nondiagonal elements. The subsystem for the diagonal elements has the form

$$\dot{\mathcal{J}}_{m'm'}=igm'(\lambda+\lambda^*)\mathcal{J}_{m'm'}-k\lambda^*\frac{\partial\mathcal{J}_{m'm'}}{\partial\lambda^*}-k\lambda\frac{\partial\mathcal{J}_{m'm'}}{\partial\lambda}+E(\lambda-\lambda^*)\mathcal{J}_{m'm'} +d_{12}(j+m')(j-m'+1)\mathcal{J}_{m'-1,m'-1}+d_{21}(j+m'+1)(j-m')\mathcal{J}_{m'+1,m'+1} -[d_{12}(j+m'+1)(j-m')+d_{21}(j+m')(j-m'+1)]\mathcal{J}_{m'm'} . \tag{21}$$

We have numerically solved the system (21) for the fourth and eleventh atoms and calculated the probability density distribution function $\mathcal{P}(\alpha)=\sum_{m'}\mathcal{P}_{m'm'}(\alpha)$, where $\mathcal{P}_{m'm'}(\alpha)=(1/\pi^2)\int d^2\lambda\exp(\lambda^*\alpha-\lambda\alpha^*)\mathcal{J}_{m'm'}(\lambda,t)$ is the probability density of finding the field in the coherent state with the amplitude α and the atom in the superpositional state $|j,m'\rangle$ (8). The real part of the field amplitude coincides with the steady-state amplitude E/k of the empty cavity: $\mathcal{P}_{m'm'}(\alpha)=\mathcal{P}_{m'm'}(y)\delta(x-E/k)$, where $\alpha=x+iy$, and therefore the distribution of the imaginary part of the field is to be calculated. The results of the numerical calculations are given in Fig. (2) ($N=4$) and Fig. 3 ($N=11$). The number of maxima of the distribution function at the fixed values g/k and d/k coincides with the number of independent excitation paths of the "quantum molecule" atoms plus field. The positions of the maxima coincide with the field amplitudes, which should be established in the cavity at its pumping by a classical field with the amplitude $E+igm'$: $\alpha=E/k+igm'/k$. Since the imaginary part of the field amplitude cannot exceed the value of $gN/2k$, then the distribution function $\mathcal{P}(y)$ is located in the range $[\alpha_{\min},\alpha_{\max}]$, where $\alpha_{\min}=E-igN/2k$ and $\alpha_{\max}=E+igN/2k$. The character of the probability distribution $\mathcal{P}(y)$ does not depend on the value of g/k; this parameter determines only the scale of the imaginary part of the field amplitude [compare Fig. 2(a) and Fig. 2(b)].

The "finesse" of the maxima of the distribution function connected with the field stability is symmetrically increased from the center towards the ends of the range [Fig. 2(a) and Fig. 3(a)], and at the fixed value d/k, it increases with the decreasing of the particle number in the system. When the ratio d/k is raised [Fig. 2(a) [3(a)] and Fig. 2(b) [3(b)]], the distribution becomes more widespread and above the critical value, depending on N, the probability density function takes the form shown in

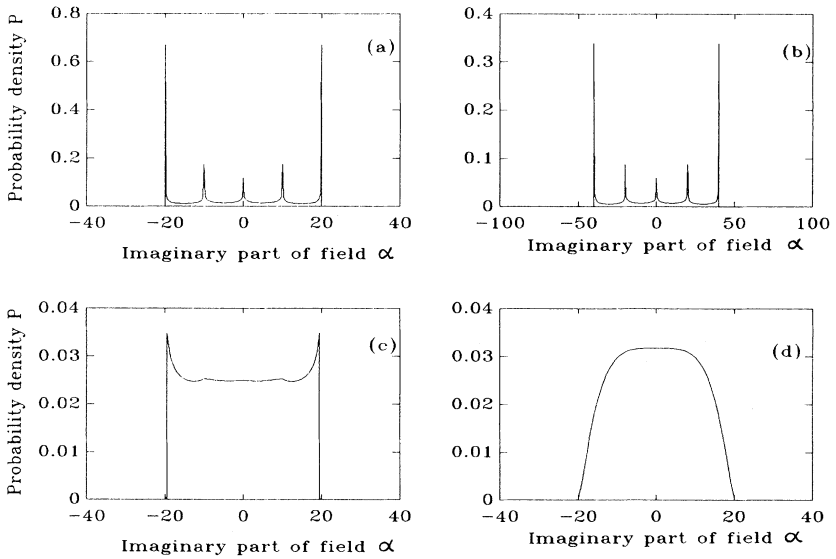

FIG. 2. $\mathcal{P}$ function of the field steady-state intracavity distribution for $N=4$ at (a) $g/k=10$, $d/k=0.05$; (b) $g/k=20$, $d/k=0.05$; (c) $g/k=10$, $d/k=0.2$; (d) $g/k=10$, $d/k=0.6$.

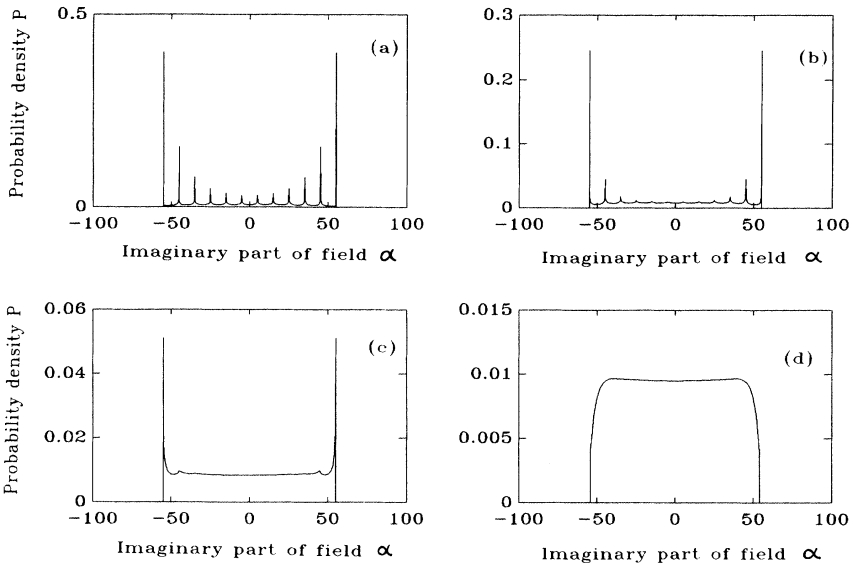

FIG. 3. $\mathcal{P}$ function of the field steady-state intracavity distribution for $N=11$ and $g/k=10$ at $d/k=0.01$ (a), $d/k=0.05$ (b), $d/k=0.1$ (c), $d/k=0.15$ (d).

Fig. 2(d) and Fig. 3(d), with a single stable state at the center of the range.

In order to find the critical value of d/k, let us assume that, with the increasing of the transition probabilities between neighbor states of the "molecule," all stable states except those corresponding to the side excitation paths disappear. In this case, it is possible to average the system (21) over the fast movements and to obtain the equations for the probability densities equivalent to a single-atom equation [8]:

$$\begin{aligned}\frac{\partial \mathcal{P}_{-j'-j'}}{\partial t}&=\frac{\partial}{\partial x}[(kx-E)\mathcal{P}_{-j'-j'}]\\&\quad+\frac{\partial}{\partial y}\left[\left[ky-\frac{gN}{2}\right]\mathcal{P}_{-j'-j'}\right]\\&\quad+d_{21}N\mathcal{P}_{j'j'}-d_{12}N\mathcal{P}_{-j'-j'}\ ,\\\frac{\partial \mathcal{P}_{j'j'}}{\partial t}&=\frac{\partial}{\partial x}[(kx-E)\mathcal{P}_{j'j'}]+\frac{\partial}{\partial y}\left[\left[ky+\frac{gN}{2}\right]\mathcal{P}_{j'j'}\right]\\&\quad-d_{21}N\mathcal{P}_{j'j'}+d_{12}N\mathcal{P}_{-j'-j'}\ .\end{aligned}\tag{22}$$

Then the conditions of appearance of at least two stable states in the system (21) are given by the inequality

$$\gamma/4k<1/N\ .\tag{23}$$

Comparing this inequality with the single-atom optical bistability inequality ($\gamma/4k<1$), we find that the collective effects in the atomic emission weaken the phase stability proportionally to the number of atoms. The solution of Eqs. (22) is given by the β-distribution law obtained in [10], with the replacement $k\rightarrow k/N$. Let us note additionally that this solution is the distribution $\mathcal{P}(y)$ averaged over all the intermediate states.

VI. ANALYTICAL SOLUTION FOR $N=2$

We successfully solved Eqs. (21) for a three-level Dicke system (two atoms in the cavity). In this case, the steady-state equations for the probability density $\mathcal{P}_{mm}$ at $m=0,\pm1$ are of the form

$$\begin{aligned}&\frac{\partial}{\partial y}[(ky-g)\mathcal{P}_{-1-1}]+2d\mathcal{P}_{00}-2d\mathcal{P}_{-1-1}=0\ ,\\&\frac{\partial}{\partial y}[ky\mathcal{P}_{00}]+2d(\mathcal{P}_{-1-1}+\mathcal{P}_{11})-4d\mathcal{P}_{00}=0\ ,\\&\frac{\partial}{\partial y}[(ky+g)\mathcal{P}_{11}]+2d\mathcal{P}_{00}-2d\mathcal{P}_{11}=0\ .\end{aligned}\tag{24}$$

It is very convenient for solving this problem to normalize the imaginary part of the field amplitude y [$z=y/(g/k)$]. The normalization removes the g/k dependence in the system (24). The role of the parameter g/k as a scale factor of the imaginary part of the field amplitude could also be demonstrated in the case of arbitrary particle number [see Eqs. (28)]. The independence of the distribution function $\mathcal{P}(y)$ on the ratio g/k is also confirmed by the numerical solution of (5).

In order to obtain the equation for the distribution function, it is necessary to take into account the following equality

$$(ky-g)\mathcal{P}_{-1-1}+ky\mathcal{P}_{00}+(ky+g)\mathcal{P}_{11}=0\ ,$$

which immediately results from Eq. (21) for the characteristic functions $\mathcal{J}_{ii}(\lambda,t)$. The normalized distribution function of the two-atom problem is found from the hypergeometric equation

$$u(1-u)\frac{d^2\mathcal{P}}{du^2}+[c-(a+b+1)u]\frac{d\mathcal{P}}{du}-ab\mathcal{P}=0\qquad(u=z^2)\ ,$$

and expressed in the following manner:

$$\mathcal{P}(x,z)=\mathcal{P}_0^{-1}\delta\left[x-\frac{E}{k}\right]\Theta(1-z^2)z^{2(1-c)}(1-z^2)^{c-a-b}\times{}_2F_1(1-a,1-b,c-a-b+1,1-z^2)\ ,\tag{25}$$

where the constants a, b, c, and $\mathcal{P}_0$ are given by the relations

$$a=\tfrac{3}{2}\left[1-2\frac{d}{k}\right], \tag{26a}$$

$$b=1-\frac{d}{k}, \tag{26b}$$

$$c=\tfrac{1}{2}\left[3-4\frac{d}{k}\right], \tag{26c}$$

$$\mathcal{P}_0=\frac{g}{2k}B(c-a-b+1,\tfrac{3}{2}-c) \times {}_2F_1(1-a,1-b,\tfrac{5}{2}-a-b;1). \tag{26d}$$

Here ${}_2F_1$ is the hypergeometric function, Θ is the Heaviside function, and B is the β-function.

The qualitative analysis of the distribution function (25) is rather simple because the $\mathcal{P}(x,y)$ function is mainly defined by its behavior in the poles $z=0,\pm1$ [see Eq. (25)], but not by the hypergeometric function ${}_2F_1$. The critical transition point for the side poles from unstable to stable states is given by the value $d/k=\frac{1}{2}$, which corresponds to the equality $c-a-b=0$. The equality $1-c=0$ ($d/k=\frac{1}{4}$) yields the critical ratio d/k for the middle stable state appearance. When $d/k<\frac{1}{4}$, the distribution has three sharp maxima in the points with the amplitudes $\alpha=E/k\pm ig/k$ and $\alpha=E/k$ (Fig. 4a).

Unfortunately, the solution in the form (25) contains the hypergeometric series that converges well only at $d/k<\frac{1}{4}$ (at $d/k>\frac{1}{4}$, it converges conditionally). For the values $d/k>\frac{1}{4}$, the distribution function can be represented in the following different form, equivalent to Eq. (25),

$$\mathcal{P}(x,z)=\mathcal{P}_0^{-1}\delta\left[x-\frac{E}{k}\right]\Theta(1-z^2)(1-z^2)^{c-a-b}\,{}_2F_1(c-a,c-b,c-a-b+1,1-z^2), \tag{27}$$

from which it follows that, for the values $d/k>1/N$ [see Eqs. (23)], the distribution $\mathcal{P}(x,z)$ has one stable point, in the middle of the range $[-1,1]$, being equal to zero on its ends.

On the basis of Eqs. (25)–(27), we have numerically calculated the distribution $\mathcal{P}(y)$ for the different values d/k. The results are presented in Fig. 4.

VII. DISCUSSION

For the elucidation of the conditions for a new stable state's appearance, let us consider the equations for the probability densities $\mathcal{P}_{m'm'}$ in the "case" of the exact resonance ($\Delta\omega=0$):

$$\frac{\partial\mathcal{P}_{m'm'}}{\partial t}=\frac{\partial}{\partial x}[(kx-E)\mathcal{P}_{m'm'}]+\frac{\partial}{\partial y}[(ky+gm')\mathcal{P}_{m'm'}] -2d(j+j^2-m'^2)\mathcal{P}_{m'm'} +d(j+m')(j-m'+1)\mathcal{P}_{m'-1,m'-1} +d(j+m'+1)(j-m')\mathcal{P}_{m'+1,m'+1}, \tag{28}$$

where $d=\gamma/4$. The phase space of the model consists of $N+1$ field phase planes that correspond to atoms being in the dressed states (8) (Fig. 5). Equations (28) describe the stochastic continuous-discontinuous Markovian process defined by the motion on phase planes along the lines $y+gm'/k=\text{const}(x-E/k)$ for the m'th plane towards the pole $x_{0m}=E/k$, $y_{0m}=gm'/k$ and by the stochastic

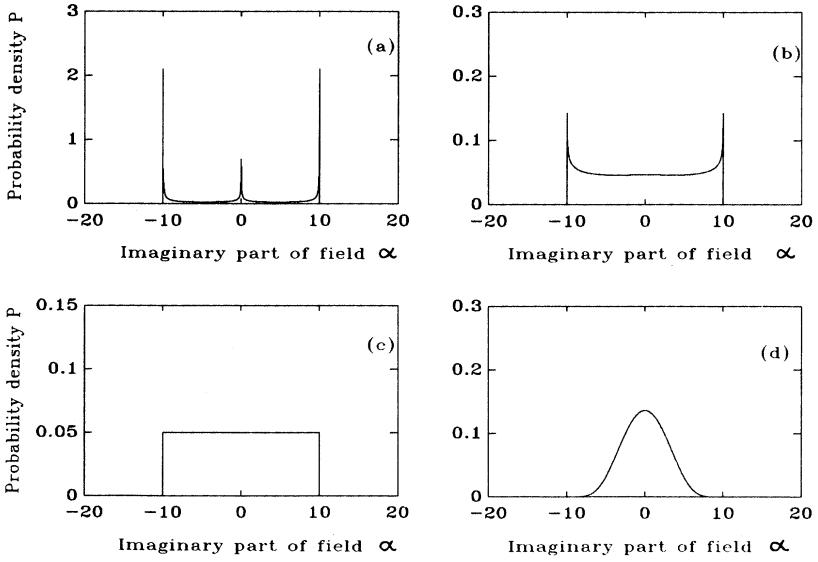

FIG. 4. $\mathcal{P}$ function of the field steady-state intracavity distribution obtained from an analytical solution of (25) and (27) for $N=2$ and $g/k=10$ at $d/k=0.1$ (a), $d/k=0.4$ (b), $d/k=0.5$ (c), $d/k=4$ (d).

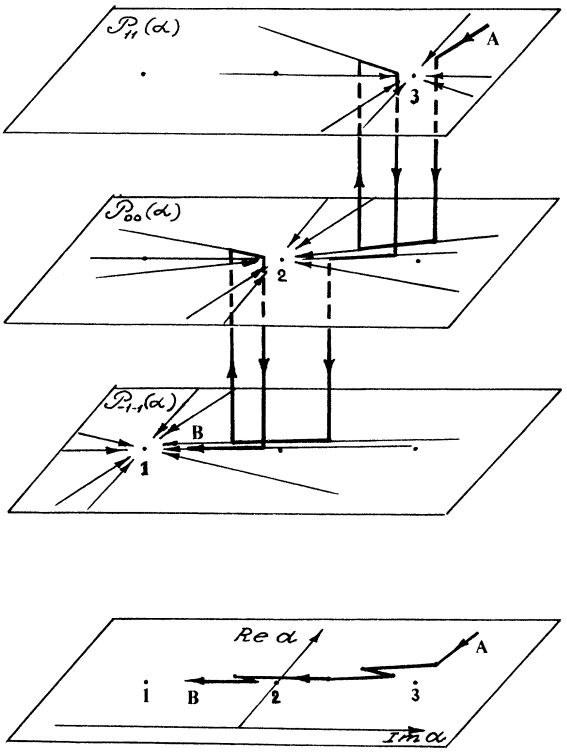

FIG. 5. (a) Stochastic evolution of the system in the phase space of the model for $N=2$. The motion on the definite plane m' corresponds to the atomic system being in the state $|j,m'\rangle$ (and to the m'th excitation path on Fig. 1). (b) Stochastic realization of the intracavity field evolution.

jumps from one plane to another according to transition probabilities. The continuous part of the Markov process is determined by the terms of Eq. (28) containing partial derivatives; the rest defines the discontinuous part of the process. On the basis of the semi-Markov-process theory, with the help of the Kolmogorov-Feller equations, one can calculate the conditional probability density $c_{m'm',nn}(t+\tau|t)$ of the next transition (jump) at time $t+\tau$ to state m', provided that, at time t, the system was in state n:

$$c_{m'm',nn}(t+\tau|t)=c_{m'n}(\tau)=d_{nm'}\exp(-\gamma_{nn}\tau) . \quad (29)$$

Here $d_{nm'}$ denotes the transition probability from plane n to the plane m', and in our case it is not equal to zero only for $m'=n\pm1$:

$$d_{n,n\pm1}=d(j\mp n)(j\pm n+1) . \quad (30)$$

The quantity $(\gamma_{nn})^{-1}$ denotes the lifetime of the state $|j,n\rangle$ ($\gamma_{nn}=\sum_l d_{nl}$) and, owing to the population balance in the system involved, it equals $\gamma_{nn}=2d(j+j^2-n^2)$.

After the nth jump at time t_n onto the m'th plane, the field amplitude is changed in accordance with

$$\alpha(t)-\alpha_{0m'}=e^{-k\langle t-t_n\rangle}[\alpha(t_n)-\alpha_{0m'}] , \quad (31)$$

where $\alpha_{0m}=E/k+igm'/k$, and k^{-1} establishes the time scale needed to achieve the steady-state point $\alpha_{0m'}$. Under the condition

$$k^{-1}\ll\Delta t<[2d(j+j^2-m'^2)]^{-1} , \quad (32a)$$

the system should be observed during the time interval Δt in the m'th, stationary state. As follows from inequality (32), at $m'=j$ the condition of the appearance of the boundary stable states (maximum stable states) coincides with (23). With decreasing m', the stability of the corresponding state is decreased, and the minimum stability is observed for the states with $m'=\pm\frac{1}{2}$ (odd number of atoms) or with $m'=0$ (even number of atoms). The inequality (32) points out the relation between parameters γ and k for a stable-state observation. If the cavity finesse is decreasing, starting from the critical value, new stable states will consecutively appear; the overall number of stable states is limited ($N+1$ states for $N+1$ atoms). The analytical solutions of a single-atom problem (critical point $d/k=1$ [10]) and a two-atom problem (critical point $d/k=\frac{1}{2}$ for $m'=\pm1$, and $d/k=\frac{1}{4}$ for $m'=0$ [6, present paper]), together with condition (21), allows us to find the general condition for critical points at an arbitrary number of the atoms:

$$2d/k(j+j^2-m'^2)=1 . \quad (32b)$$

As seen from Eq. (31), the stochastic trajectory of the Markov process after a few jumps will be restricted by the range $[\alpha_{\min},\alpha_{\max}]$ (see Fig. 6). When the condition (32b) is not achieved, the system moves rapidly between the poles that are nearest to the central one. Therefore, it can be mainly found in the central point of the trajectory. In the case of multistability, the system spends most of the time near one of the poles. The values of the field amplitude corresponding to the stable states are presented in Fig. 6. All points of the phase trajectory have the same real part of the field amplitude E/k, and an imaginary part increasing as the arithmetic series with the step g/k, beginning from the minimum value $-jg/k$. Besides the difference of phases between the input field and one of the values of the output field

$$\varphi_{m'}=\arctan(gm'/E) , \quad (33)$$

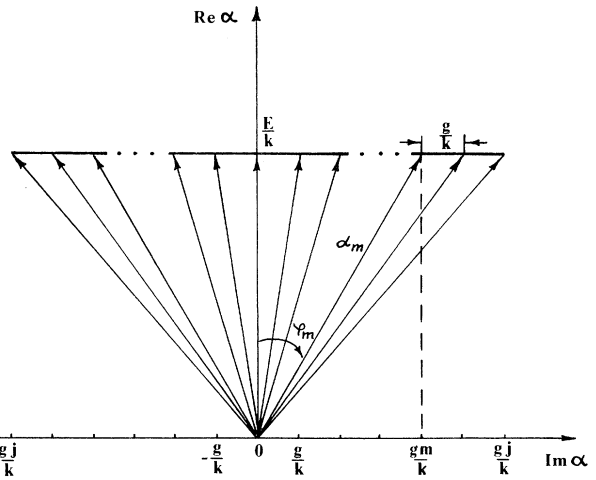

FIG. 6. Diagram of the stationary values of the intracavity field complex amplitude for the even number of atoms.

the difference in modulus

$$\Delta|\alpha_{m'}|=E/k\{[1+(m'g/E)^2]^{1/2}-1\} \quad (34)$$

appears, which permits us to refer to the predicted effect as the amplitude-phase multistability. Note that, at $N\rightarrow\infty$, the maximum phase difference tends to $\pi/2$.

Thus, the predicted multistability may be experimentally observed by comparison of the amplitudes and the phases of the input and output fields, e.g., using the interference phenomena. However, it should be taken into account that, for observing all possible stable states, the observation time $\Delta T\sim\sum_{m'=-j}^{j}[2d(j+j^2-m'^2)]^{-1}$ is needed.

VIII. POSSIBLE EXPERIMENT

The experimental conditions of the amplitude-phase multistability observation are more accessible than those of a single-atom bistability [10]. In the multiatom experiment, the cavity finesse can be reduced in N times compared with the single-atom case under the conditions of high pump intensity, strong coupling for the execution of inequality (9), and the conservation of the boundary-state stability. The observed phase difference will surpass the difference $\Delta\varphi$ for the single-atom problem in $[\arctan(gN/2E)]/\arctan(g/2E)$ times.

As was shown previously, two conditions [Eq. (9) and Eq. (32)] should be fulfilled for an experimental realization of the predicted effect. Both of them can be achieved in the modern experimental devices. For example, in [15] the effect of absorptive bistability has been investigated in the case of strong interaction of the atomic Cs ($\lambda_{D_2}=852$ nm) beam with the field of the high-quality cavity with the transmitting coefficient $T_0=4\times10^{-5}$ [$k=cT_0/2L=2\pi(0.9\pm0.1)$ MHz, $L=1$ mm]. The coupling constant g_0 was of the same order as the spontaneous emission probability γ: $[g_0,\gamma]=[2\pi(3.2\pm0.2,\ 5\pm0.4)]$ MHz. The normalized input pump intensity $Y=I_{\text{in}}/(I_sT_0)\sim10^4$ (titanium–sapphire laser with the beam waist $\omega_0=50$ μm), where $I_s=1$ mW/cm^2, $I_i/I_0=(c/4)(\hbar\omega/\pi\omega_0^2L)(E/k)^2$, gives the estimation of the Rabi frequency of the atomic oscillations in experiment [15] as $\Omega\sim10^2g$, that allows the conditions (9) to be fulfilled. However, in this experiment, the inequality (32) is not achieved due to the large value of the ratio γ/k. But this inequality can be easily satisfied. Therefore we conclude that at least the effect of single-atom optical phase *bistability* is realizable in the case of conditions that are close to the conditions of experiment [15].

As for observing the effect of amplitude-phase *multistability*, the atoms should be confined in the region small compared with the resonant wavelength during the time interval Δt defined by Eq. (32). This is a more complicated experimental problem. But some collectively radiating systems can be proposed: a system of atoms in optical traps, colliding beams of atoms, and a system of atoms formed by a molecule dissociation (see, for example [16,17]). Besides that, a molecule with a semiequidistant energy spectrum could also be a candidate for the generation of amplitude-phase multistable light.

In conclusion, it should be noted that the effect of multistability of the two-level atomic system in a high-Q cavity reflects the quantum character of the atomic interaction with radiation to a larger extent than the effect of a single-atom phase bistability considered in [10,11]. If the effect of a single-atom phase bistability could be explained on the basis of the quasiclassical model by interpreting the creation of two stable states as an appearance of stationary points on the Bloch sphere [10], then for the explanation of the internal stability states in the case of an atomic system, such an approach, based on the equations for the mean values $\langle J_i\rangle$, could not be used. On its basis, one can only explain the existence of two boundary stationary states. The appearance of the internal stable states demands for their explanation the consistently quantum approach, which is not restricted by the lowest-order means $\langle J_i\rangle$.

ACKNOWLEDGMENT

The authors are grateful to the Belorussian Fundamental Foundation for the financial support (Grant No. F4-027).

APPENDIX

Let us consider the structure of the energy levels for the multiparticle analog of the Jaynes-Cummings Hamiltonian [14] in the case of exact resonance $\omega=\omega_0$

$$H=\hbar\omega a^\dagger a+\hbar\omega J_z+\hbar g(a^\dagger J_-+aJ_+)\ . \quad (A1)$$

The eigenvectors of the Hamiltonian (A1) can be expressed as $|n-j-m\rangle_f|m\rangle_a$, where indices f and a label the eigenstates of the free resonator field and atomic system, respectively. As shown in [14], the interaction Hamiltonian $\hbar g(a^\dagger J_-+aJ_+)$ has the eigenstates

$$|2j,n,r\rangle=\sum_{m=-j}^{k}\alpha_m^n|n-j-m\rangle_f|m\rangle_a\ , \quad (A2)$$

where the number $n=0,1,2,\ldots$ corresponds to the excitation number in the system "field plus atoms,"

$$k=\begin{cases}j\ , & \text{when } n\geq 2j\ ,\\ n-j\ , & \text{when } n<2j\ .\end{cases}$$

The number r, varying from $-n/2$ to $n/2$ at $n<2j$ and from $-j$ to j when $n\geq2j$, enumerates the eigenstates of the Hamiltonian $\hbar g(a^\dagger J_-+aJ_+)$ belonging to the fixed number of excitation n. The states $|2j,n,r\rangle$ are also the eigenstates of the Hamiltonian H with the energy eigenvalues

$$\mathcal{E}_{2j,n,r}=\hbar\omega(n-j)+E_{2j,n,r}\ , \quad (A3)$$

where $E_{2j,n,r}$ are the eigenvalues of the interaction Hamiltonian

$$\hbar g(a^\dagger J_-+aJ_+)|2j,n,r\rangle=E_{2j,n,r}|2j,n,r\rangle\ . \quad (A4)$$

According to (A2) and (A4), the coefficients α_m^n satisfy the recurrent equation

$$\alpha_{m+1}^nS_m^n-E_n\alpha_m^n+\alpha_{m-1}^nS_{m-1}^n=0\ , \quad (A5a)$$

with the boundary conditions

$$\alpha^n_{-j-1}=\alpha^n_{j+1}=0\ ,\quad n\geq 2j\ ,$$
$$\alpha^n_{-j-1}=\alpha^n_{n-j+1}=0\ ,\quad n<2j\ , \tag{A5b}$$

and the eigenvalues E_n are defined from the equation

$$\det{}^n_{-j}=\begin{vmatrix} -E & S^n_{-j} & 0 & \cdots & 0 & 0 & 0 \\ S^n_{-j} & -E & S^n_{-j+1} & \cdots & 0 & 0 & 0 \\ 0 & S^n_{-j+1} & -E & \cdots & 0 & 0 & 0 \\ \cdots & & & & & & \\ 0 & 0 & 0 & \cdots & S^n_{k-1} & -E & S^n_k \\ 0 & 0 & 0 & \cdots & 0 & S^n_k & -E \end{vmatrix} =0\ , \tag{A6}$$

where $S^n_m=\hbar g\sqrt{(n-j-m)(j+m+1)(j-m)}$ and $E\equiv E_{2j,n,r}$. The dimension of matrix (A6) sets the number of split sublevels of the free Hamiltonian energy level $E_{0n}=\hbar\omega(n-j)$ at given n and j. The number of sublevels corresponding to the level E_{0n} grows proportionally to the excitation number n (Fig. 1). The maximum of sublevels is restricted by the maximum dimension of matrix (A6) and equals $2j+1$. With further increasing of the excitation number, only the distance between split levels increases.

Using the recurrent equation for $\det^n_{-j}$ obtained by the decomposition of the determinant (A6) on the element of the first line

$$\det{}^n_{-j}=E\det{}^n_{-j+1}-(S^n_{-j})^2\det{}^n_{-j+2}\ , \tag{A7}$$

we obtain that, in the case of even dimension of matrix (A6), the splitting on sublevels E_n is symmetrical relative to E_{0n}, but in the case of odd dimension, besides the symmetrical sublevels, the level with $E_{2j,n,0}=0$ is available. The corresponding scheme of the energy levels for the even ($2j\equiv N=2$) or odd ($2j\equiv N=3$) number of atoms is presented in Fig. 1(a) [Fig. 1(b)].

In the case of large excitation number n, e.g., at the large number of photons

$$n\gg 2j\ , \tag{A8}$$

it is possible to obtain the approximate solution of Eqs. (A15) and (A16). Indeed, assuming in Eqs. (A5a) $S_m\approx\hbar g\sqrt{n}\sqrt{(j+m+1)(j-m)}$, we obtain that Eqs. (A5a) are equivalent to the eigenvalue problem

$$\hbar g\sqrt{n}\,(J_++J_-)|\psi_E\rangle=E|\psi_E\rangle\ , \tag{A9}$$

where

$$|\psi_E\rangle=\sum_{m=-j}^{j}\alpha^n_m|m\rangle_\alpha\ , \tag{A10}$$

and $|m\rangle_a$ are the eigenstates of operator J_z. The solution of Eq. (A9) is obvious. Performing the rotation transformation

$$J'_z=\exp\left[i\frac{\pi}{2}J_y\right]J_x\exp\left[i\frac{\pi}{2}J_y\right]\ , \tag{A11}$$

we obtain that, in the considered approximation, the eigenstates E up to a factor coincide with the eigenstates of the angular-momentum operator J'_z

$$E_{2j,n,r}=2\hbar g\sqrt{n}\,r\quad(r=-j/2,\ldots,j/2)\ , \tag{A12}$$

and eigenvectors $|\psi_E\rangle$ are connected with eigenvectors $|r\rangle\equiv|m'\rangle$ of operator J'_z via the equation

$$\exp\left[-i\frac{\pi}{2}J_y\right]|\psi_E\rangle=|r\rangle\ . \tag{A13}$$

According to the last equation, the coefficients α^n_m are defined by Wigner d functions and, at $n\gg 2j$, they are independent of the excitation number n:

$$\alpha^n_m=d^j_{mr}(-\pi/2)\ . \tag{A14}$$

Thus, the approximate eigenstates of the interaction Hamiltonian at large n have the form

$$|2j,n,r\rangle\approx\sum_{m=-j}^{j}d^j_{mr}(-\pi/2)|n-j-m\rangle_f|m\rangle_\alpha\ . \tag{A15}$$

Under the action of the input field [the interaction Hamiltonian $iE(a^\dagger-a)$], the system "atoms plus intracavity field" can perform the transitions between the states $|2j,n,r\rangle$. The matrix transition elements are equal to

$$\langle 2j,n',r'|a|2j,n,r\rangle=\langle 2j,n',r'|\sum_{m=-j}^{j}d^i_{mr}(-\pi/2)\sqrt{n-j-m}\,|n-j-m-1\rangle_f|m\rangle_\alpha\sqrt{n}\,\delta_{n',n-1}\delta_{r,r'}\ . \tag{A16}$$

Consequently, at $n\gg 2j$, the transitions between the states with the same quantum number r only are allowed. This explains the existence of $2j+1$ independent excitation paths. Moreover, taking into account that, for calculating the mean values of field operators at $n\gg 2j$, one can use the approximate matrix elements (A16), the eigenstates (A15) can be represented in the factorized form

$$|2j,n,r\rangle\approx|n\rangle_f|r\rangle_\alpha\ , \tag{A17}$$

where the states $|r\rangle_\alpha=\sum_{m=-j}^{j}d^j_{mr}(-\pi/2)|m\rangle_\alpha$ coincide with the dressed states (8) at $\varphi=\pi/2$.

[1] R. H. Dicke, Phys. Rev. **93**, 99 (1954).
[2] M. S. Feld, and J. C. MacGillivray, in *Coherent Nonlinear Optics,* edited by M. S. Feld and V. S. Letokhov (Springer-Verlag, Berlin and New York, 1980).
[3] S. Ya. Kilin [Sov. Phys. Zh. Eksp. Teor. Fiz. **78**, 2157 (1980) JETP **51**, 1081 (1980)].
[4] R. R. Puri and S. V. Lawande, Phys. Lett. **72**, 200 (1979).
[5] S. Ya. Kilin, J. Phys. B **13**, 2653 (1980).
[6] G. S. Agarwal, L. M. Narducci, and E. Apostolidis, Opt. Commun. **36**, 285 (1981).
[7] S. Ya. Kilin [Sov. Phys. Zh. Eksp. Teor. Fiz. **82**, 63 (1982) JETP **55**, 38 (1982)].
[8] R. Bonifacio and L. A. Lugiato, Opt. Commun. **19**, 172 (1976).
[9] C. M. Savage and H. J. Carmichael, IEEE J. Quantum Electron. **24**, 1495 (1988).
[10] S. Ya. Kilin and T. B. Krinitskaya, J. Opt. Soc. Am. B **8**, 2289 (1991).
[11] P. Alsing and H. J. Carmichael, in *Optical Society of America Proceedings on Nonlinear Dynamics in Optical Systems,* edited by N. B. Abraham, E. M. Garmire, and P. Mandel (Optical Society of America, Washington, DC, 1990), Vol. 7.
[12] R. R. Puri, G. P. Hildred, S. S. Hassan, and R. K. Bullough, in *Optical Bistability 2,* Proceedings of the International Topical Meeting on Optical Bistability, edited by C. M. Bowden, H. M. Gibbs, and S. L. McCall (Plenum, New York, 1983).
[13] E. P. Wigner, *Group Theory and its Application to the Quantum Mechanics of Atomic Spectra* (Academic, New York and London, 1959).
[14] M. Tavis and F. W. Cummings, Phys. Rev. **170**, 379 (1968).
[15] J. Rempe, R. J. Thompson, R. J. Brecha, W. D. Lee, and H. J. Kimble, Phys. Rev. Lett. **67**, 1727 (1991).
[16] P. Grangier, A. Aspect, and J. Vigue, Phys. Rev. Lett. **54**, 418 (1985).
[17] G. Kurizki, G. Hose, and A. Ben-Renven, Phys. Rev. A **38**, 6433 (1988).